Available online at www.sciencedirect.com
ScienceDirect
European Journal of Pharmaceutics and Biopharmaceutics 68 (2008) 828–837
European Journal of Pharmaceutics and Biopharmaceutics
www.elsevier.com/locate/ejpb

Research paper

Monitoring galenical process development by near infrared chemical imaging: One case study

C. Gendrin [a,b,*], Y. Roggo [a], C. Spiegel [a], C. Collet [b]

[a] F. Hoffmann-La Roche A.G., Basel, Switzerland
[b] LSIIT – UMR CNRS 7005, Strasbourg University, France

Received 14 June 2007; accepted in revised form 3 August 2007
Available online 10 August 2007

Abstract

The objective of this study is to evaluate by NIR imaging the homogeneity of process intermediates obtained with different process parameters during the development of a new pharmaceutical solid form. The process under investigation is a solid dosage form based on extrusion. The parameters are two kinds of crystallizations, two sizes of particle of API, two screw speeds during the extrusion and two milling screens used to reduce the extrudates into a granulate form. Two kinds of intermediates are evaluated: the extrudates and the cores. Two approaches are used to analyze the data: the univariate NIR analysis which consists in wavelength selection and multivariate analysis, i.e., Classical Least Squares (CLS), which takes into account the whole spectra. The univariate method reveals good chemical homogeneity of the extrudates but differences in their physical aspect. CLS shows well-distributed excipients for all the cores; differences in the sizes of the granules have also been revealed. The univariate method can be applied on simple chemical systems such as binary mixtures. When complex samples are analyzed, multivariate analysis is the method of choice. This study demonstrates that NIR imaging can be a useful tool for the optimization of the process and for the selection of the final parameters of the process.

Keywords: Near infrared imaging; Process Analytical Technology; Galenical development; Multivariate analysis; Extrusion; Homogeneity

1. Introduction

Process understanding has become an important goal for the pharmaceutical industry. Controlling and mastering the different process phases allows a constant quality of the drugs, a decrease in the number of rejected batches and a shorter time to market [1]. Therefore, since 2002, the Food and Drug Administration (FDA) has promoted the development of science based techniques that can be integrated throughout the manufacturing line to ensure final product quality. This initiative is called "Process Analytical Technology" (PAT) [2].

In this context, vibrational spectroscopy including Raman, Infrared and Near Infrared (NIR) spectroscopy has experienced renewed interest in the past few years. These techniques allow the monitoring of reaction [3], the characterization of raw materials [4] and polymorphic forms [5], as well as the monitoring of crystallization [6], and drying [7]. NIR has been particularly used as an analytical technique to assess the powder blend uniformity [8], to quantify API (Active Pharmaceutical Ingredient) content [9] or to characterize differences between pharmaceutical batches [10]. Recently, detectors allowing the acquisition of multiple spatially located NIR spectra at the same time so as to provide spectral images have been developed to visualize the compound distributions. These detectors, named FPA (Focal Plan Array), are combined with Tunable Filters for the selection of the wavelength and with several objectives to provide several spatial resolutions and fields of view. The association of imaging for spatial localization and

* Corresponding author. F. Hoffmann-La Roche A.G., Grenzacherstrasse, 65/516, PTGF-Q ABPS, CH-4070 Basel, Switzerland. Tel.: +41 616886502.
E-mail address: christelle.gendrin@roche.com (C. Gendrin).

0939-6411/$ - see front matter © 2007 Elsevier B.V. All rights reserved.
doi:10.1016/j.ejpb.2007.08.008

spectroscopy for the characterization of the compound is referred to as chemical imaging [11]. The pharmaceutical industry is particularly interested in this technique since it makes it possible to map chemical distributions for assessing the homogeneity of the samples [12,13] and to quantify API [14,15].

During the development of new pharmaceutical products, several parameters such as mixing time or API/excipient variants have to be tuned in order to find the optimum formulation which would allow good bio-availability and the more efficient cost production. Each of the batches resulting from this campaign is subsequently analyzed by classical techniques such as for instance among other analytical techniques, sieve analysis, to assess the particle size distribution of the intermediate materials, HPLC for content analysis, dissolution test, in order to evaluate the quality of the tablets and measure the influence of the parameters. One of the other main issues is the homogeneity of the samples and NIR imaging appears to be an adequate tool for this task because it is rather fast and gives information about the spatial localization of the chemical species in tablets.

The aim of this paper is therefore to demonstrate, by the help of a particular case study, how NIR imaging can actually be used to understand the process during the development of a product and to help in the choice of final process parameters. In this study, the influence of four different parameters on the homogeneity of two process intermediates is under investigation. The homogeneity of the sample is assessed by NIR-Chemical Imaging (NIR-CI) by using two different processing techniques: univariate and multivariate analysis.

2. Materials

2.1. Process and samples

The process under investigation is based on extrusion which increases the drug solubility by dispersing the API in a polymer matrix. The extrusion is defined by J. Breitenbach [16] as "a process of converting a raw material into a product of uniform shape and density by forcing it through a die under controlled conditions". For more information on extrusion the reader is referred to [16].

The process workflow is constituted of six main steps and two kinds of process intermediates are taken along the line. The first step is the mixing in a blender of the API with a polymer which acts as the matrix for the solid dispersion. The powder blend is then passed through the extruder. The first samples are withdrawn after cooling of the extruded material (the extrudates). The material is subsequently milled through a Fitz Mill to form a granulate. Other excipients are added and the powder is mixed until homogeneity of the material is reached. The mixture is then compressed with a tabletting machine into cores, which are the second process intermediates. Fig. 1 summarises up the different steps of the production and figures out the sampling during the process.

2.2. Parameters under investigation

During the extrusion phase, several parameters, such as screw speed and API variants, may influence the homogeneity of the extrudate and these parameters have

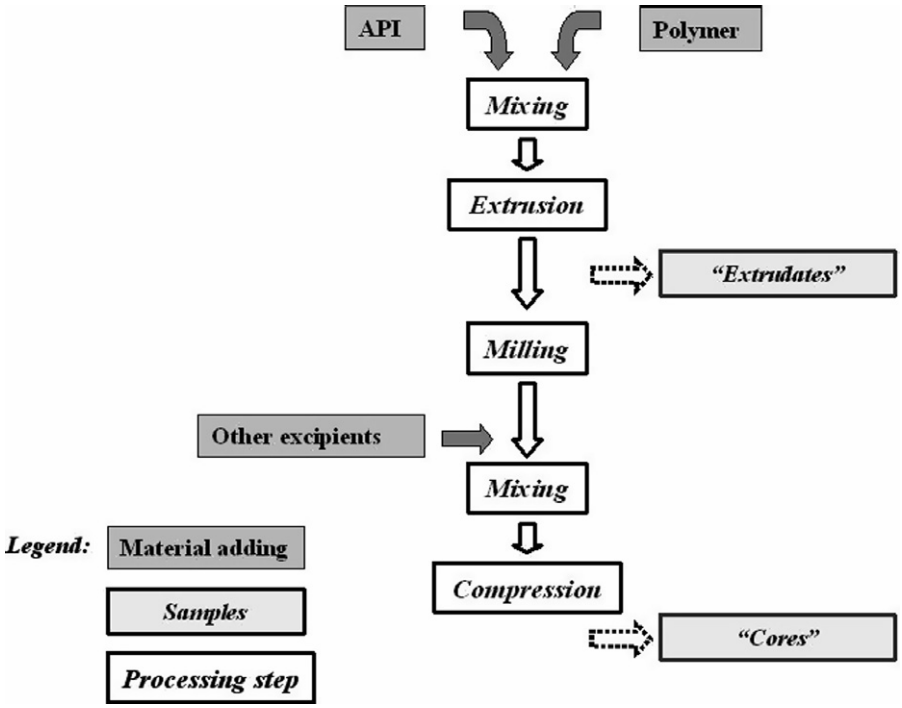

Fig. 1. Process workflow and sampling procedure.

to be carefully chosen. Therefore, the first two parameters concerned the API morphology. Two types of API crystallizations were used. For each API crystallization, two different particle size distributions were produced. One variant featured large particles whereas the other one presented finer ones.

The last two parameters were process parameters. Two different screw speeds during the extrusion were compared as well as two different milling screens.

Eight extrudates, ten granulates and ten cores were then analyzed. Fig. 2 sums up the different process parameters and associated samples used in the study.

2.3. Samples preparation

For the analysis, the extrudates were simply laid down on a mirror plate. The cores were trimmed according to their length by the help of a tungsten bevel-edge milling blade (Leica EM trim), in order to flatten the analyzed surface.

2.4. Powder references

In order to know the chemical signature of each of the compounds which constituted our samples, the pure powders of each of the species (API, polymer, excipient 1, excipient 2, excipient 3) were also scanned by our hyperspectral imager. Thus, the reference spectra are acquired in the same experimental conditions as the samples.

2.5. NIR imaging system

The samples and the powder references were analyzed with the Sapphire® near-infrared imaging system marketed by Malvern (Worcestershire, United Kingdom). The detector size is 320×256 pixels allowing the simultaneous acquisition of 81920 spectra.

The acquisition parameters were 16 co-adds and a spectral range of 1000–2450 nm at 10-nm increments. Extrudates and cores were imaged with the objective 40 μm/pixel providing a field of view of $1 \times 1.3\ cm^2$ allowing the analysis of the whole surface of the tablet. One measurement is about 5 min.

2.6. Softwares

Data were acquired with the SaphireGo software. Preprocessing and first investigation of the data were made with Isys® v3.1. The Matlab software (v7.1 The Mathworks, www.mathworks.com) was used to perform multivariate analysis.

3. Methods

3.1. Live images

During the acquisition, the chemical imaging system provides the real time image at a chosen wavelength. It is possible to acquire these images called "live images". As they reveal physical aspects of the samples it is interesting to compare these images. For the study the wavelength 1930 nm which corresponds to the O—H bond was selected. This wavelength provides high contrast images because the detector signal is at its maximum.

3.2. Hyperspectral data cube preprocessing

The spectra acquired by the system are reflectance spectra. Therefore, the inverse logarithm, $\log_{10}(1/R)$, was first applied to the data cube to convert the spectra in absorbance unit. A mask was applied in order to remove pixels which are from the background.

The spectra were normalized by the help of the Standard Normal Variate in order to remove scattering effects. Then, a

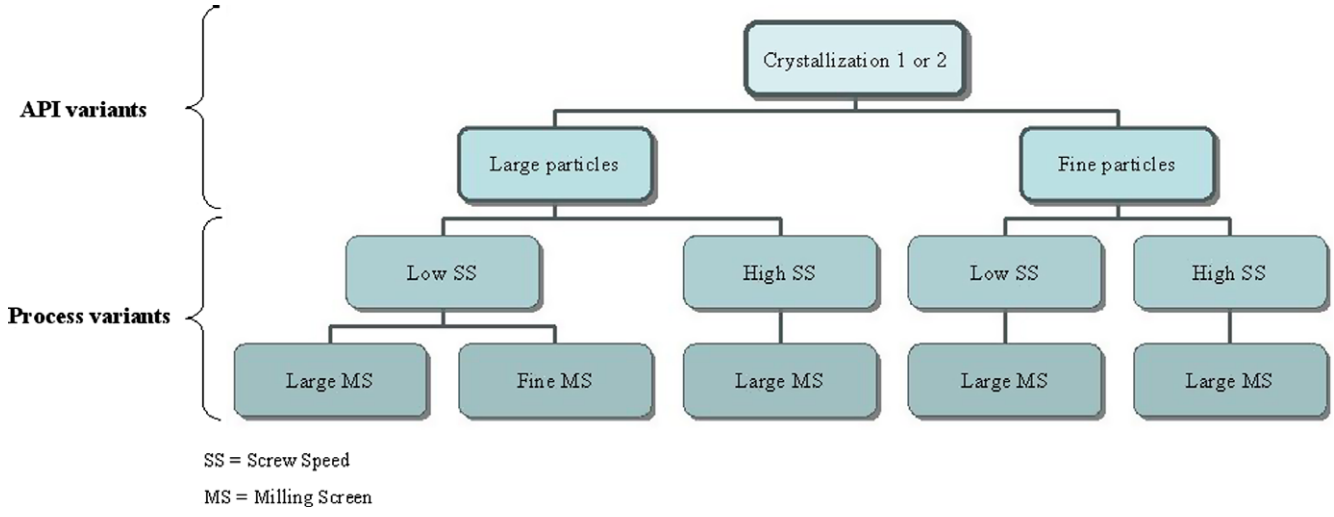

Fig. 2. Sample plan – Design of experiments.

Savitzky-Golay second derivative (filter order 3, filter width 9) of NIR data was computed to enhance spectral variations due to chemical species and to correct the baseline.

3.3. Univariate analysis

3.3.1. Wavelength selection

The imaging system provides three dimensional data cube which needs to be processed in order to get relevant spatial and spectral information. The univariate analysis consists in the study of the compound distribution at a specific wavelength. It was applied to analyze the first process intermediate: the extrudates. The wavelengths are chosen by finding the characteristic peaks of the chemical species by the help of the preprocessed reference spectra. After preprocessing of the data cube, the selected image shows the distribution of each pixel intensity at that wavelength.

Wavelength 2180 nm was chosen as API characteristic wavelength and the wavelength 2260 nm was chosen as the polymer one for study of the extrudates. Those two wavelengths were chosen because they can clearly be attributed to one of the compounds when looking at the preprocessed reference spectra (cf Fig. 3) and also because they provide the best contrast in the images.

3.3.2. Histogram comparison

In order to evaluate the homogeneity of the samples, histograms of the image at polymer specific wavelength were analyzed. Histogram represents the distribution of the pixel values in the image. Three statistical parameters were computed to quantify their differences [11]. Those three parameters are extracted:

- First the mean value of the distribution is estimated:

$$\hat{\mu} = \frac{1}{n}\sum_{i=1}^{n} x_i$$

  where n represents the total number of pixels within the image and x_i the value of the pixel i.
- Secondly their variance

$$\hat{\sigma}^2 = \frac{1}{n-1}\sum_{i=1}^{n}(x_i - \hat{\mu})^2$$

- And finally the kurtosis which gives information about the shape of the histogram peak

$$\hat{k} = \frac{\frac{n(n+1)}{(n-1)(n-2)(n-3)}\sum_{i=1}^{n}(x_i - \hat{\mu})^4}{\sigma^4}$$

3.4. Multivariate analysis

The bilinear model is used to achieve the extraction of the distribution maps in the second process intermediate. The procedure to extract the distribution maps is displayed in Fig. 4. After unfolding the data cube ($x * y * \lambda$) into a two-dimensional matrix $\mathbf{X} = ((x * y) * \lambda)$, the method consists in decomposing the matrix $\mathbf{X}$ into the product of two

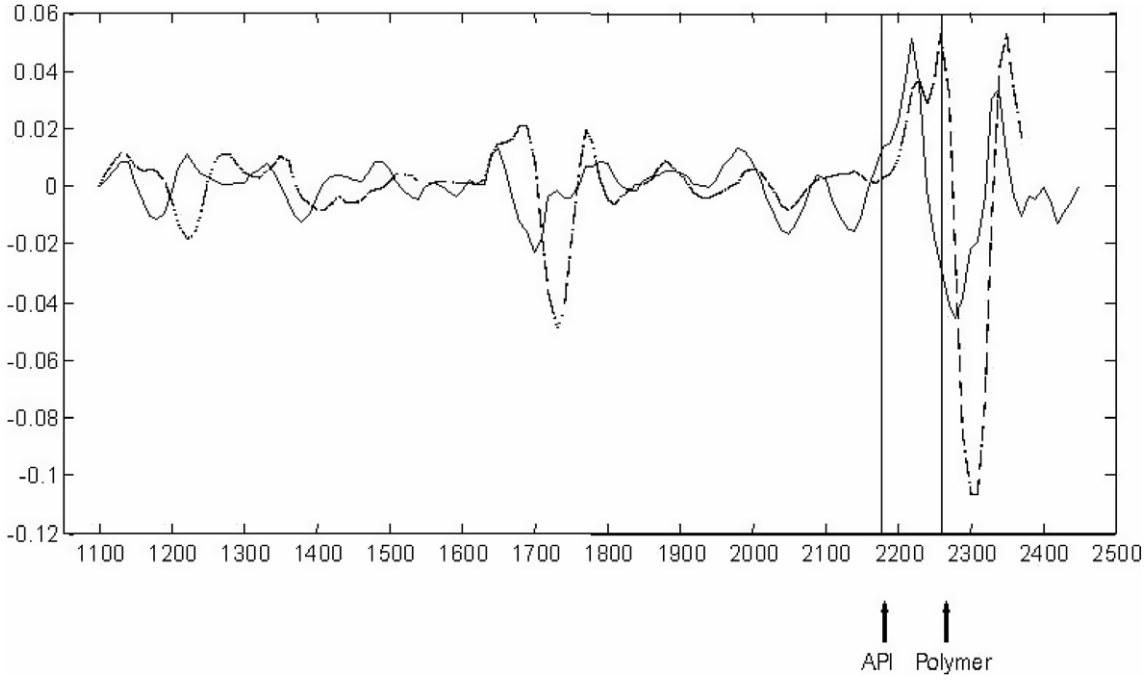

Fig. 3. API and polymer reference spectra with specific wavelength positions. The wavelengths at 2180 nm (API) and 2260 nm (polymer) were chosen to display univariate images.

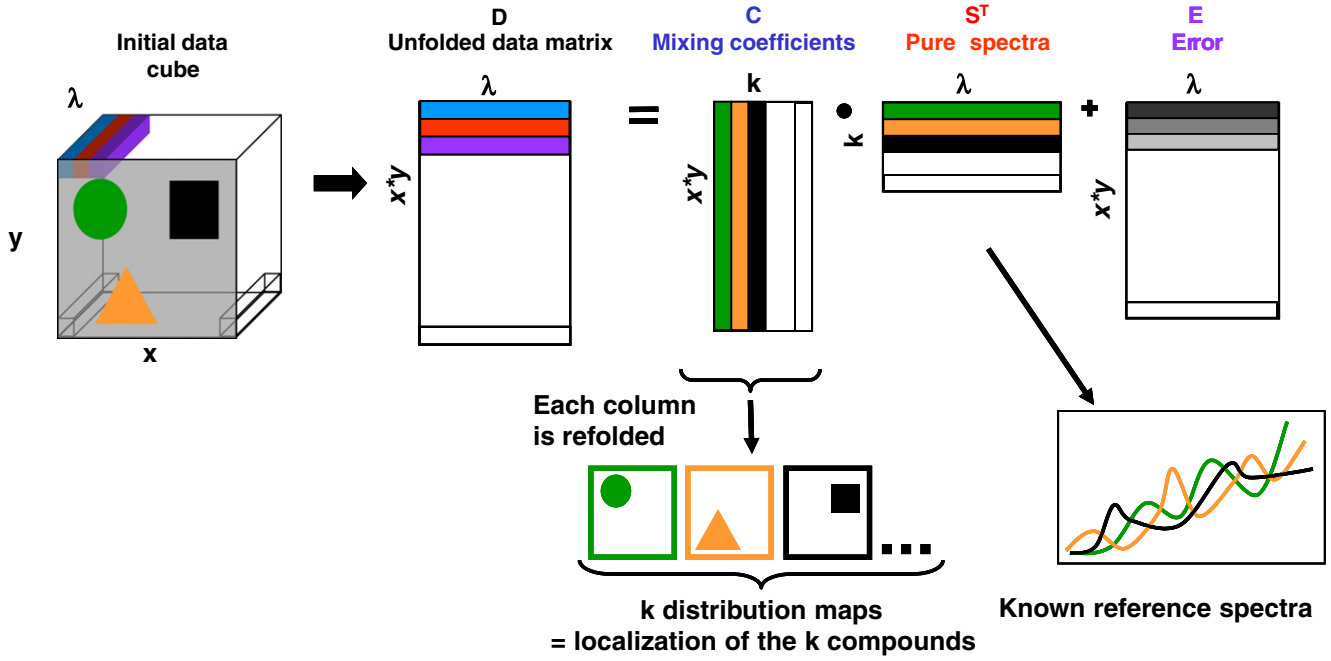

Fig. 4. Extraction of the distribution maps using the bilinear model and CLS algorithm.

matrices, $\mathbf{C}$ and $\mathbf{S}^{\mathbf{T}}$: $\mathbf{X} = \mathbf{C}\mathbf{S}^{\mathbf{T}} + \mathbf{E}$, where $\mathbf{E}$ is the matrix which counts for experimental errors. The rows in $\mathbf{S}^{\mathbf{T}}$ contain the pure compound signals, the columns in $\mathbf{C}$ contain their related concentration profiles or unfolded distribution maps.

As the reference spectra of the chemical species constituted the sample are known, Classical Least Squares (CLS) algorithm is performed to extract the matrix $\mathbf{C}$. This method consists in the minimisation of the sum of the square errors, i.e., the minimisation of $\|\mathbf{X}\text{-}\mathbf{C}\mathbf{S}^{\mathbf{T}}\|$, with the matrix $\mathbf{S}^{\mathbf{T}}$ containing the reference spectra. At the end, the distribution map corresponding to the compound $\mathbf{S}_{\mathbf{i}}^{\mathbf{T}}$ is obtained by refolding back the corresponding column $\mathbf{C}_i$.

4. Results and discussion

4.1. Extrudate samples

Fig. 5 displays the "live image" obtained with the extrudates. Differences in the physical aspect can visually be pointed out. First, the screw speed influenced the extrudate smoothness. Actually, by comparing extrudate A with B, extrudate C with D, extrudate E with extrudate F, we can conclude that the higher the screw speed is, the more irregularities appear on the extrudate surface. Regarding the API variants, extrudates formed with large API particles present flakes and a more rough surface (A, B, E, F) whereas the extrudates using fine API particles seem to be more homogeneous especially for extrudates C, G, H. Finally, the fine API particles of crystallization 2 produce the smoothest extrudates and this formulation is less sensitive to screw speed (physical aspects of extrudates G and H are quite similar).

"Live images" reveals physical differences in the samples but the link with chemical meaning is not obvious and conclusions about compound distributions can only be made after processing of the data and chemical characterization. Figs. 6 and 7 depict the extrudates at specific wavelengths. The first one is an image at API specific wavelength (2180 nm) and the second one is at a polymer specific wavelength (2260 nm). Characteristic wavelength images represent the distribution of pixel intensity which corresponds to signal intensity at that particular wavelength. Those images are false-color images. Red (white in gray-level image for paper version) represents high intensity pixels and blue (black in gray-level image for paper version) represents low intensity pixels. Intermediate intensity values are represented with intermediate colors linearly distributed between blue and red according to the visible spectrum (or gray-level for paper version), as shown on the color bar displayed on the right of the figures. At a specific wavelength, the high intensity pixels (i.e., red pixels) are therefore linked to a higher content of the associated chemical specie.

It can be visually noticed that a high intensity in the image at 2180 (Fig. 6) corresponds to a low intensity at 2260 nm (Fig. 7) and vice versa: the images are complementary. Therefore, it can be concluded that the chosen wavelengths in our case are able to discriminate between the two compounds, one image being characteristic of one of the compounds.

Inhomogeneity between the two constituent distributions is clearly visible in the extrudate B. Effectively, the images at 2260 nm reveal large spots of red color which is linked to a higher content of polymer at these locations (higher pixel intensity) whereas at 2180 nm it corresponds

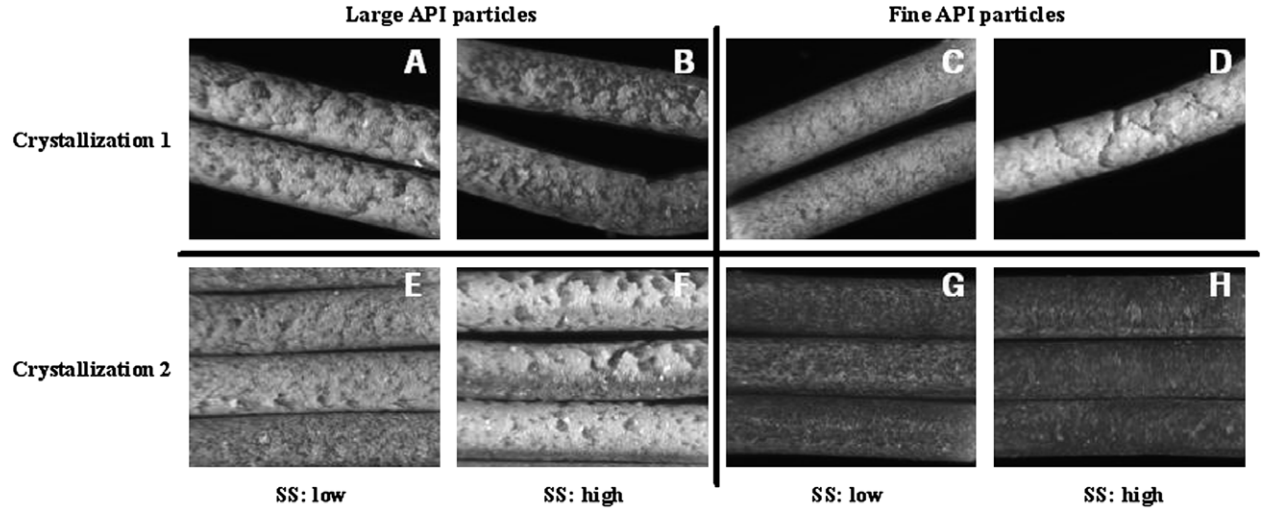

Fig. 5. Extrudate live images at 1930 nm (O—H bonds). The screw speed influences the extrudate smoothness: the higher the screw, the more irregularities appear on the surface. Extrudates produced with fine API particles are also smoother (images C, G, H) than the ones produced with large API particles. SS, screw speed.

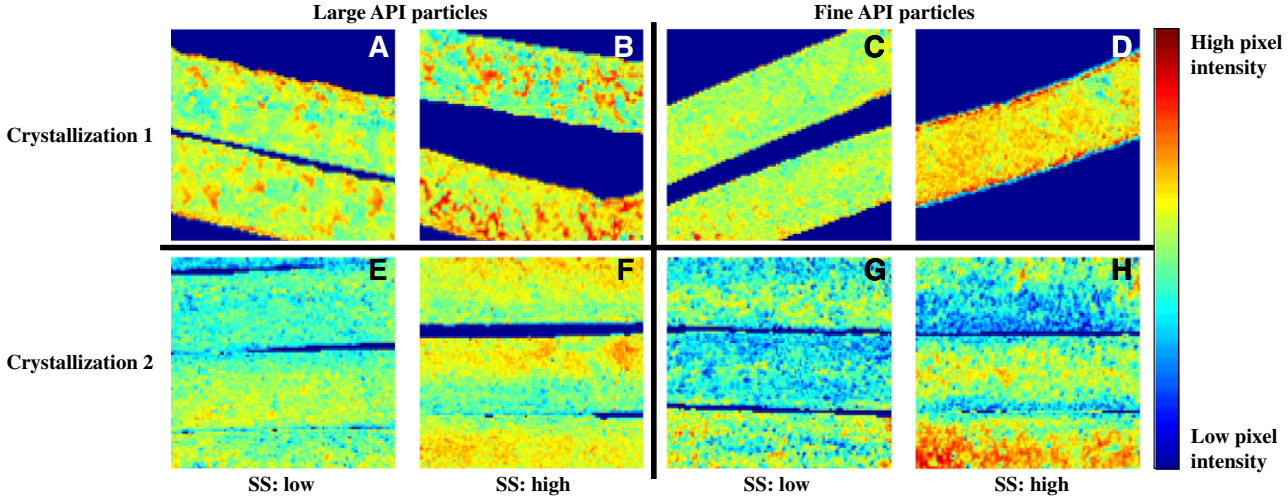

Fig. 6. Extrudates at API specific wavelength (2180 nm). SS, screw speed.

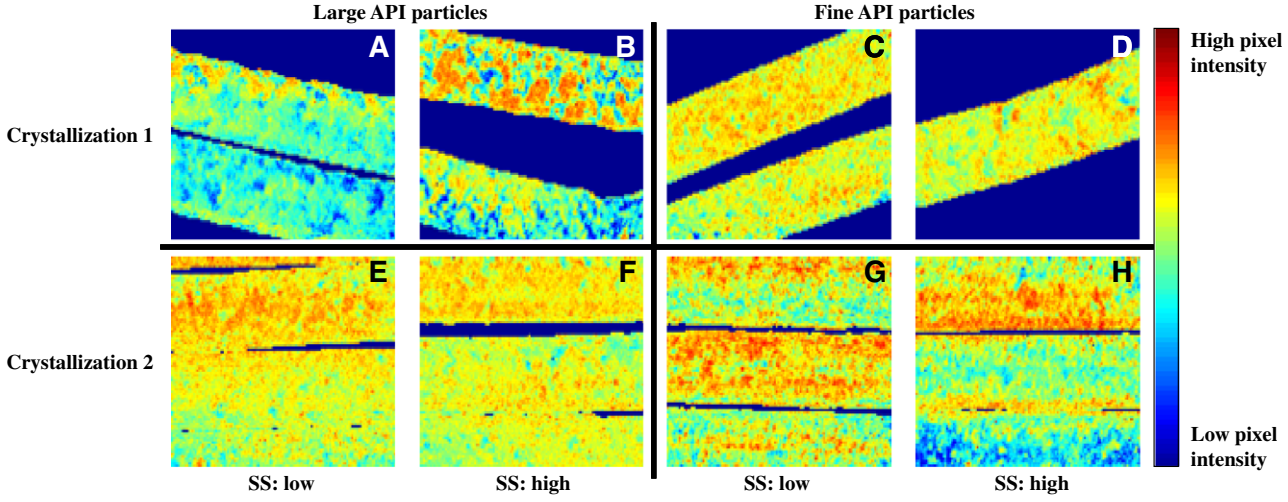

Fig. 7. Extrudates at polymer specific wavelength (2260 nm). Image B shows the more heterogeneous sample. SS, screw speed.

to lower pixel intensities (lower API content). In the other batches the intensities are rather distributed uniformly on the sample surface which are then homogeneous.

This interpretation can be confirmed by considering the histogram of each image. An histogram which exhibits a symmetric distribution with a narrow base and a sharp peak is representative of an image with a low contrast, therefore an homogeneous sample. On the other hand an asymmetric histogram with a large base and flatter peak is representative of contrasted image therefore heterogeneous sample. Fig. 8 displays the histograms of the images at the polymer characteristic wavelength and Table 1 gives their related statistics. The variance is representative of the base shape whereas the kurtosis is representative of the peak shape. The higher the variance the larger the base; the higher the kurtosis, the sharper the peak. The histograms A C D E F have a similar distribution, i.e., narrow base and lower variance; sharp peak and higher kurtosis which are representative of an homogeneous sample.

Images B, G, H exhibit the broader distributions and peaks. This is confirmed by the statistics, their variance are larger and their kurtosis lower. Finally, the histogram analysis confirms that image B is the more heterogeneous with a variance of 0.33×10^{-4} and a kurtosis of 2.75.

Those results lead to the conclusion that the screw speed and API forms have an effect on the physical appearance of the extrudates and their homogeneity. Especially, the batch B exhibits heterogeneous distribution in both the live image and the images at specific wavelengths. On the other side, it was reported during the extrusion that the feed rate of the extruder, i.e., the speediness of the material entering the extruder, does not vary when screw speed increases with crystallization 1, whereas it increases proportionally with crystallization 2 (probably due to a higher bulk density of the API crystallization 2). Therefore, our hypothesis is that crystallization 1 produces less dense extrudates leading to rougher surface of the extrudates. Moreover, the NIR imaging study at characteristic wavelengths reveals, that crystallization 1 leadss to heterogeneous extrudates (image

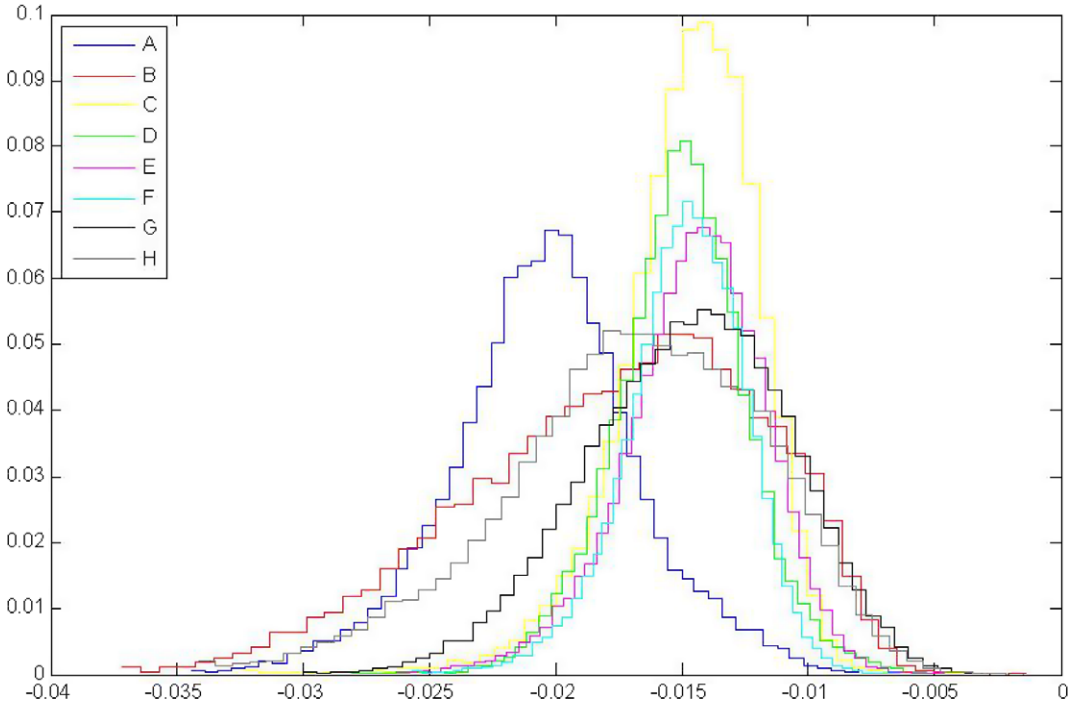

Fig. 8. Histograms of extrudate images at polymer specific wavelength. Histograms A, C, D, E, F exhibit a symmetric distribution with narrower base and sharper peaks than histograms B, G, H. This is characteristic of a low contrasted image and therefore the compound distribution is more homogeneous for these samples. Histogram B presents the largest base and flatter peak, the image features then the more heterogeneous sample.

Table 1
Statistics related to the histograms of images at polymer specific wavelength

	A	B	C	D	E	F	G	H
Mean	−0.021	−0.08	−0.015	−0.0153	−0.0147	−0.0151	−0.0151	−0.0173
Variance	0.143	0.332	0.076	0.069	0.078	0.057	0.158	0.263
Kurtosis	.058	2.7566	5.74	3.84	3.59	3.86	2.89	3.06

Histogram B presents the larger variance and lower kurtosis.

B) which should therefore be avoided. Other considerations such as dissolution and technical aspects lead to use the conditions of the batch G or H for the production. NIR imaging can then support this choice because the extrudates are regular and present good homogeneity.

4.2. Core images

Fig. 9 displays the live images from the core. Differences in the sizes of the granules are revealed. Considering especially images A1 vs A2 differences due to the size of the milling screen can be pointed out: A1 which was produced with a large milling screen has larger granule sizes than A2. The granule sizes changed also for the crystallization 1 when the screw speed increased: see images A1 vs B and C vs D. The higher the screw speed, the finer the particles. This phenomenon is less evident for crystallization 2.

Using multivariate analysis is necessary to identify chemically the particles inside the cores. Effectively, when the number of chemical compounds is increasing in the samples, finding a specific wavelength for each compound is a critical task, and multivariate analysis which takes into account the information containing in the whole spectrum is more adequate to the problem. Fig. 10 shows the distribution maps of the granulates within the cores extracted by the help of the CLS algorithm. The multivariate analysis confirms that the black particles which appeared in the live image are actually granules of the milled extrudate, and the difference in their sizes pointed out above is still visible.

The granule sizes were also assessed by sieving directly after the milling step. Those results showed finer granules for samples B and samples D, which correlate with the qualitative analysis of the cores under NIR lamps. The difference in the granule sizes can be compared with the observations made with the extrudates. One can notice that the cores which contain the smaller ones correspond to the rougher extrudates (samples B and D). The authors assume that, those extrudates are more friable and can therefore lead to finer granules during the milling step.

Fig. 11 displays the distribution maps of the excipients inside the tablet of batch A1. The distribution maps in the other tablets of the study were quite similar, therefore they are not displayed here. It can be visually noticed that homogeneous distribution is obtained for the excipients. Excipient 1 is rather uniformly distributed in the tablet. Excipients 2 and 3 formed agglomerates as the spots in the distribution maps are up to 1 mm width whereas the initial powders do not feature such large particles. However, these spots are uniformly distributed inside the cores. Thus, NIR imaging analysis revealed no differences between the distribution of excipients inside the cores which is confirmed by the fact that no process variants were done with the excipients, with the final blending or with the compression of the blend into tablets in this study. However, it was not possible to extract information about minor compounds, because they represent less than 1% of the final weight of the tablet and are under the detection limit of the apparatus.

4.3. NIR imaging advantages

The advantages of NIR imaging are that one measurement of about 5 min is able to give spatial and chemical information about the samples and the large field of view provides a good overview of the tablets.

The live image, taken at 1930 nm, provides a very high contrast which was not achievable with classical visible images (author observations, images not shown here). They reveal the physical aspect of the sample. For this study, the granules inside the cores appear clearly and it was possible to notice differences in their size in correlation to screw speed for crystallization 1. Obviously, the granule size distribution within final cores cannot be assessed by classical method such as sieving without destroying the cores. It can be assessed right after the milling step, but it is not sure that,

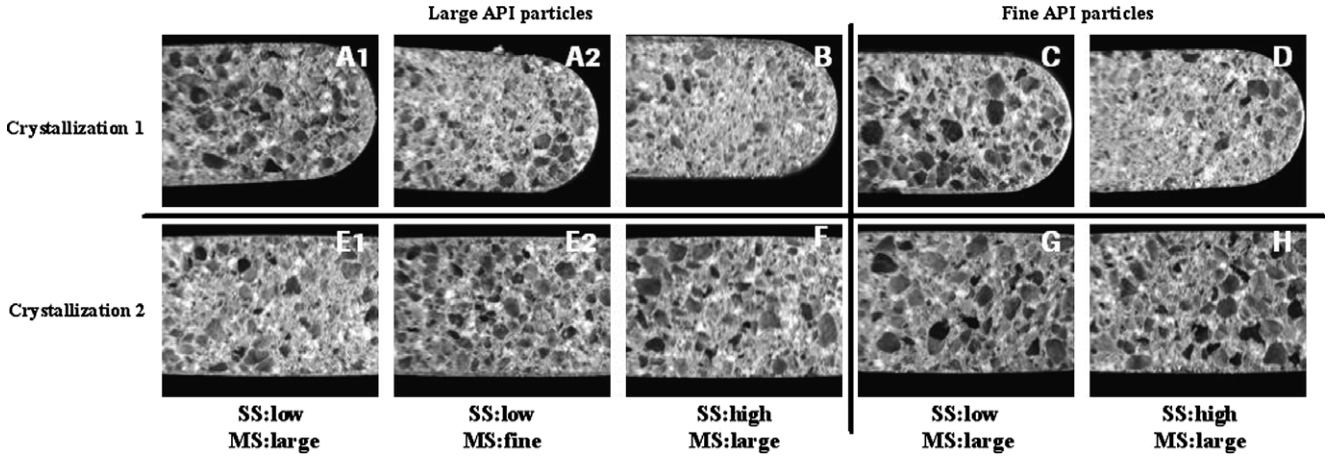

Fig. 9. Core live images. Differences in particle sizes between image A1 and B, C and D can be pointed out. This suggests that for the crystallization 1 the screw speed influense the particle sizes: the higher the screw speed, the finer the particles. SS, screw speed; MS, milling screen.

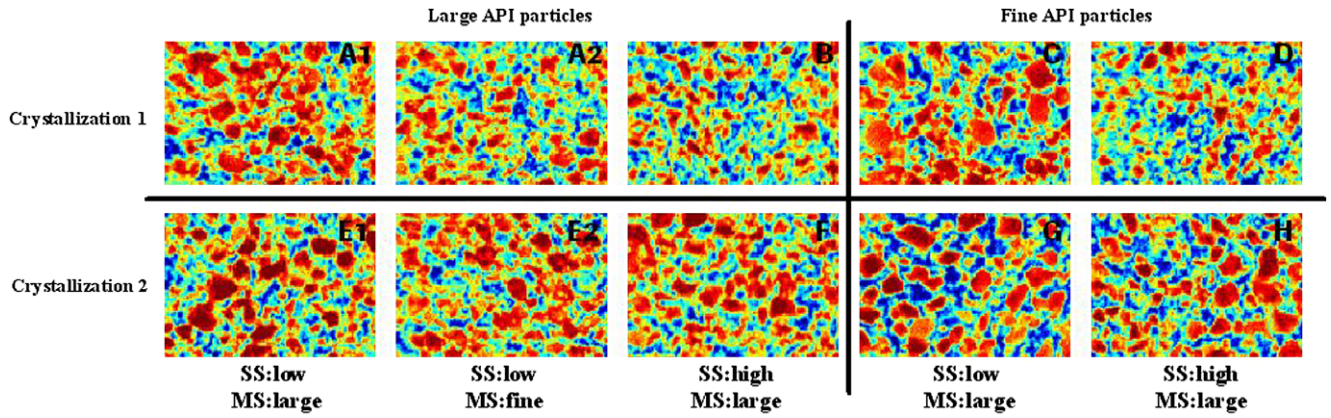

Fig. 10. Granulate distribution maps inside the tablets (zoom on the center of the tablets). The distribution maps are homogeneous. The black particles seen in the live image are particles of the milled extrudates. SS, screw speed; MS, milling screen.

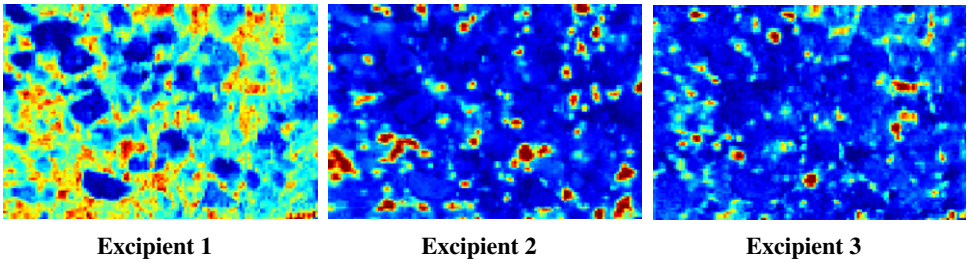

Fig. 11. Distribution maps of the excipients within batch A1 (zoom on the center of the tablet).

during compression, no new aggregation of those granulates occurs. NIR image analysis is therefore an alternative solution to assess particle size distribution in final product.

After processing of the data, NIR imaging allows clear identification and localization of the chemical species of the samples. Univariate analysis, as well as multivariate analysis, extracts the relative distribution maps, and conclusions about homogeneity can be drawn up. Inside the cores, the agglomeration of the excipient is revealed and according to the author's knowledge, no other classical method can provide this information. It is possible to assess the homogeneity of the binary mixture of API and polymer before extrusion and the final blend before compression by regular sampling at different places inside the blender with the help of sample thieve and content analysis but it is not sure that chemical species after extrusion and after compression are uniformly distributed inside the intermediates. In this study, it was demonstrated that the extrudates of batch B are inhomogeneous. The inhomogeneity is rather fine and would not have been noticed by the classical sampling method. NIR imaging is therefore a method of choice to check the distribution of the chemical species inside solid intermediates and tablets.

5. Conclusions

It is shown in this study that NIR imaging appears to be a valuable analytical technique to be used in parallel with other classical methods for the analysis of samples produced during the development of a new drug formulation and to help in the choice of the parameters of the process. The advantages of the imaging technique are that it is fast, it requires little preparation of the samples, and above all provides information about the localization of the compound and their identification. Both univariate and multivariate processing are required to extract relevant information from the data sets. In the case study, the analysis of the samples taken all along the line reveals good homogeneity of the material and supports the final choice of the parameters.

Moreover, systematic analysis of samples generated during the development by NIR imaging allows the creation of a database with known parameters which may be useful later as a reference for potential investigations of product failures. It also allows the development of routines and algorithms dedicated for the specific product, thus enabling faster analysis of the future samples.

References

[1] K.A. Bakeev, Process Analytical Technology, Blackwell Publishing, Oxford, 2005.
[2] http://www.fda.gov/cder/OPS/PAT.htm.
[3] K. Braekeleer, A. Juan, F.C. Sanchez, P.A. Hailey, D.C.A. Sharp, P. Dunn, D.L. Massart, Determination of the end point of a chemical synthesis process using on-line measured mid-infrared spectra, Appl. Spectrosc. 54 (2000) 601–607.

[4] M. Blanco, A. Eustaquio, J.M. Gonzalez, D. Serrano, Identification and quantitation assays for intact tablets of two related pharmaceutical preparations by reflectance near-infrared spectroscopy: validation of the procedure, J. Pharm. Biomed. Anal. 22 (2000) 139–148.
[5] G. Buckton, E. Yonemochi, J. Hammond, A. Moffat, The use of near infra-red spectroscopy to detect changes in the form of amorphous and crystalline lactose, Int. J. Pharm. 168 (1998) 231–241.
[6] G. Fevotte, J. Calas, F. Puel, C. Hoff, Applications of NIR spectroscopy to monitoring and analyzing the solid state during industrial crystallization processes, Int. J. Pharm. 273 (2004) 159–169.
[7] T.P. Lin, C.C. Hsu, Determination of residual moisture in lyophilized protein pharmaceuticals using a rapid and non-invasive method: near infrared spectroscopy, PDA J. Pharm. Sci. Technol./PDA 56 (4) (2002) 196–205.
[8] M. Blanco, R. Gozalez Bano, E. Bertran, Monitoring powder blending in pharmaceutical processes by use of near infrared spectroscopy, Talanta 56 (2002) 203–212.
[9] P. Chalus, Y. Roggo, S. Walter, M. Ulmschneider, Near-infrared determination of active substance content in intact low-dosage tablets, Talanta 66 (2005) 1294–1302.
[10] Y. Roggo, C. Roeseler, M. Ulmschneider, Near infrared spectroscopy for qualitative comparison of pharmaceutical batches, J. Pharm. Biomed. Anal. 36 (2004) 777–786.
[11] Neil Lewis, Joseph Schoppelrei, Eunah Lee, L. Kidder, Near-infrared chemical imaging as a process analytical tool, in: K.A. Bakeev (Ed.), Process Analytical Technology, Blackwell, London, 2005, pp. 187–225.
[12] F. Clarke, Extracting process-related information from pharmaceutical dosage forms using near infrared microscopy, Vib. Spectrosc. 34 (2004) 25–35.
[13] Y. Roggo, A. Edmond, P. Chalus, M. Ulmschneider, Infrared hyperspectral imaging for qualitative analysis of pharmaceutical solid forms, Anal. Chim. Acta 535 (2005) 79–87.
[14] J. Burger, P. Geladi, Hyperspectral NIR imaging for calibration and prediction: a comparison between image and spectrometer data for studying organic and biological samples, Analyst 131 (2006) 1152.
[15] C. Gendrin, Y. Roggo, C. Collet, Content uniformity of pharmaceutical solid dosage forms by near Infrared hyperspectral imaging: a feasibility study, Talanta (2007), doi:10.1016/j.talanta.2007.04.054.
[16] J. Breitenbach, Melt extrusion: from process to drug delivery technology, Eur. J. Pharm. Biopharm. 54 (2002) 107–117.